**Zeitschrift:** Helvetica Physica Acta

**Band:** 63 (1990)

**Heft:** 3

**Artikel:** Quasiparticles and photoemission spectra in correlated fermion systems

**Autor:** Horsch, Peter

**DOI:** https://doi.org/10.5169/seals-116225

**Nutzungsbedingungen**

Die ETH-Bibliothek ist die Anbieterin der digitalisierten Zeitschriften auf E-Periodica. Sie besitzt keine Urheberrechte an den Zeitschriften und ist nicht verantwortlich für deren Inhalte. Die Rechte liegen in der Regel bei den Herausgebern beziehungsweise den externen Rechteinhabern. Das Veröffentlichen von Bildern in Print- und Online-Publikationen sowie auf Social Media-Kanälen oder Webseiten ist nur mit vorheriger Genehmigung der Rechteinhaber erlaubt. Mehr erfahren

**Conditions d'utilisation**

L'ETH Library est le fournisseur des revues numérisées. Elle ne détient aucun droit d'auteur sur les revues et n'est pas responsable de leur contenu. En règle générale, les droits sont détenus par les éditeurs ou les détenteurs de droits externes. La reproduction d'images dans des publications imprimées ou en ligne ainsi que sur des canaux de médias sociaux ou des sites web n'est autorisée qu'avec l'accord préalable des détenteurs des droits. En savoir plus

**Terms of use**

The ETH Library is the provider of the digitised journals. It does not own any copyrights to the journals and is not responsible for their content. The rights usually lie with the publishers or the external rights holders. Publishing images in print and online publications, as well as on social media channels or websites, is only permitted with the prior consent of the rights holders. Find out more

**Download PDF:** 08.01.2026

**ETH-Bibliothek Zürich, E-Periodica, https://www.e-periodica.ch**

Helvetica Physica Acta
Vol. 63 (1990)

0018-0238/90/030345-19$1.50+0.20/0
(c) 1990 Birkhäuser Verlag, Basel

# QUASIPARTICLES AND PHOTOEMISSION SPECTRA IN CORRELATED FERMION SYSTEMS

Peter Horsch

Max-Planck-Institut für Festkörperforschung

D-7000 Stuttgart 80, Federal Republic of Germany

## ABSTRACT

Results obtained for the single-particle Greens function by analytical and numerical methods are discussed for various models presently under consideration for the electronic structure of high-temperature superconductors (HTSC). The numerical calculation of photoemission spectra is performed for small systems by using the Lanczos method.

For the Emery model (extended Hubbard model for the $CuO_2$-planes) photoemission and inverse photoemission spectra for the insulating (undoped) and for doped cases are discussed. High-energy satellites and new low-lying excitations in the charge-transfer energy gap appear as a consequence of the strong Coulomb correlations on the Cu-sites. These low-energy states appear to be responsible for conductivity and superconductivity in hole-doped HTSC's. The atomic character of these states and their spin-correlations is examined.

The relation to the one-band Hubbard and the t-J model is reviewed and a detailed discussion of the spectral functions for these models is presented. In particular we investigate the effect of the next-nearest neighbor hopping terms which appear in order $t^2/U$ and which are frequently discarded in the derivation of the t-J Hamiltonian. Supercells up to 18 sites are studied numerically and the fundamental difference between one and two dimensions is elucidated. In 2D we find evidence for a coherent quasiparticle band of width 2J with a dispersion relation $E_{\vec{k}} \sim \frac{J}{2}(\cos k_x + cosk_y)^2$ and $S = 1/2$, which emerges at the low energy edge of the otherwise incoherent spectrum.

Finally we compare the single-particle excitation spectrum of the t-J model with the low-lying excitations of the Emery-model.

## INTRODUCTION

Excitation spectra of strongly-correlated electronic systems are even more difficult to calculate than ground state properties. In such cases the problem is often first simplified by a further reduction of the model Hamiltonian, and (or) by searching for reasonable approximations. The method of exact diagonalization of finite clusters can be of great value in this process, as approximations may be more rigorously tested than is otherwise possible. We present here calculations of the single particle (hole) excitation spectrum of extended Hubbard models but also for the t-J model. This provides a direct comparison of the physical content of these models and actual photoemission and inverse photoemission spectra (PES) of high-temperature superconductors (HTSC).

Considerable insight into the electronic structure and the nature of the charge carriers in HTSC comes from various types of photoemission and inverse photoemission experiments [1] . Such experiments showed that the states close to the Fermi level in the metallic samples have strong oxygen character, i.e. additional holes go essentially on oxygen. Recent investigations of the O 1s absorption edge [2,3] showed that the oxygen orbitals contributing to these states have 95% $p_{x,y}$-symmetry, with x and y in the plane [3] . By angle resolved photoemission in superconducting $Bi_2CaSr_2Cu_2O_8$ even a band crossing the Fermi level could be resolved [4,5] . A Fermi edge has been seen by several groups, which has subsequently been interpreted as indicating Fermi liquid behaviour. A further success of this class of spectroscopies was the observation of the superconducting gap by high-resolution UV-photoemission [6] .

The theoretical difficulty with HTSC's is their closeness to Mott-Hubbard insulators. The undoped reference materials such as $La_2CuO_4$ and $YBa_2Cu_3O_6$ are antiferromagnetic insulators [7,8] . Standard bandstructure calculations predict metallic behavior instead, with no tendency towards antiferromagnetism [9] . Bandstructure theory also fails to explain photoemission, e.g. satellite structures at high energy, because the single particle picture no longer provides a valid description. This is well known for the transition metal oxides [10] , and suggests that the underlying physics has certain similarities. Under these circumstances it is evident that electronic correlation effects must be taken into account properly to achieve an understanding of the electronic properties of these materials. Due to the complexity of the many-body problem at hand present theoretical studies of HTSC's are still limited to simple models for the electronic structure.

The 3-band Hubbard (Emery) model [11] which includes both Cu and O degrees of freedom is expected to contain the features discussed above. There is still controversy whether the 3-band model can be reduced to an effective one-band model, which describes the physics at low energy in the doped case. Zhang and Rice [12] suggested that a local singlet formed by a hole on Cu and a dopant hole distributed over 4 neighboring O($p_\sigma$) orbitals leads for certain parameter choices again to an effective single band model.

There seems to exist agreement that the magnetic properties of the undoped system are well described by the isotropic spin-1/2 Heisenberg model [13], viz. the atomic limit of the 1-band Hubbard model at half-filling. This is a direct consequence of the strong correlations on the Cu-sites, that is the stabilization of the Cu $d^9$-configuration. The fact that doping destroys long-range antiferromagnetic order at rather low concentration of holes (3% in $La_{2-x}Sr_xCuO_4$) is a direct indication of the strong coupling between the holes and the Cu-spins. I discuss here the reverse question, namely the effect of the spin-system on the nature of the carriers. That is the spectral function of a hole in an Heisenberg antiferromagnet (t-J model).

The method used to calculate the spectral function is a generalization of the recursion method of Haydock, Heine and Kelly [14] based on the Lanczos algorithm, which has previously been used in a many-body context by Gunnarsson and Schönhammer [15] and others [16,17,18]. It is remarkable that the Lanczos method retains its good convergency known for the lowest eigenstates also for rather complex spectra as in the case of the Emery model. This provides a direct comparison of the physical content of these models and the outcome of approximation schemes.

This contribution is organized as follows. After a description of the numerical approach to the calculation of spectral functions, I consider the photoemission and inverse photoemission spectra obtained for the 3-band model. Particular emphasis will be put on the characterization of the low-lying excitations in this model. The next topic is the spectral function of a hole in the t-J model. Finally I conclude by comparing the low-energy physics of the Emery model and the excitation spectrum of the t-J model.

## CALCULATION OF THE SPECTRAL FUNCTION

The spectral density of the single-hole excitations may be defined as

$$A_{k\sigma}(\omega) = \frac{1}{N_c}\sum_m |\langle\psi_m(N-1)|a_{k\sigma}|\psi_0(N)\rangle|^2\delta(\omega - E_0(N) + E_m(N-1)). \quad (1)$$

Here the operator $a_{k\sigma}$ annihilates a particle with momentum $k$ and spin $\sigma$, $|\psi_0(N)\rangle$ is the ground state eigenfunction of an N-particle system, and $|\psi_m(N-1)\rangle$ is an eigenstate of the (N-1)-particle system, which have energies $E_0(N)$ and $E_m(N-1)$, respectively. An analogous definition applies for the particle spectral function. Naturally momentum conservation restricts the possible final states $|\psi_m(N-1)\rangle$ which may contribute to the spectral function. The hole spectral function may be rewritten as imaginary part of the single-particle Greens function:

$$A_{k\sigma}(\omega) = \frac{1}{\pi} Im\langle u_0(N-1)|\frac{1}{E+H-i\delta}|u_0(N-1)\rangle, \quad (2)$$

where $|u_0(N-1)\rangle = a_{k\sigma}|\psi_0(N)\rangle$, and $E = \omega - E_0(N)$ is the excitation energy measured from the ground state energy of the $N$-particle system, and $\delta \to 0^+$. In

practice a finite value of $\delta$ leads to a useful smoothing of the spectra, which would otherwise consist of a set of spikes due to the relatively small number of k-points used.

The desired expectation value is readily calculated iteratively by using the Lanczos algorithm to generate a basis in which the Hamiltonian is tri-diagonal. To begin with the N-particle ground state eigenvector $|\psi_0(N)\rangle$ is calculated using the standard Lanczos technique. Then a particle is annihilated in this state in a fashion which may depend on the experiment which is being mimicked when there is more than a single site per unit cell. This new (N-1) -particle state is then expressed in the appropriate basis, and the problem of calculating the propagator has been reduced to the evaluation of the expectation value of the matrix $(H+z)^{-1}$ in this state $|u_0(N-1)\rangle$. The desired expectation value may be found by renewed application of the Lanczos algorithm, with the starting vector given by $|u_0(N-1)\rangle$. After $M$ Lanczos iterations, an $M$ dimensional tridiagonal representation of the Hamiltonian is generated. The coefficients of this matrix may then be used in a continued-fraction expansion [14] of the inverse $(H+z)^{-1}$, or equivalently this expectation value may be expressed in terms of the eigenvalues and eigenvectors of the (small) $M$-dimensional tridiagonal matrix. The latter approach is to be preferred if frequency integrals over the density of states are desired.

## EMERY MODEL

The bandstructure of a typical HTSC [19] looks rather complicated, nevertheless essential features can be expressed in a simple 3-band tight-binding model [20] . The problem is thought to simplify firstly because there is only one electron per $CuO_2$ unit cell missing to fill all bands. Secondly the largest overlap is between Cu($d_{x^2-y^2}$) and O($p_\sigma$)- orbitals in the Cu-O planes. These orbitals have a relatively small energy separation $\epsilon = \epsilon_p - \epsilon_d$, leading to strong covalent splitting of the corresponding bands. The resulting bands form the top and the bottom of the band complex, and the topmost anti-bonding band is half-filled. Apart from the bonding and antibonding band there is a nonbonding band which is dispersionless as long as the direct hopping matrix element $t_{pp}$ between oxygens is zero.

The Coulomb interaction is characterized by 3 terms, a Hubbard repulsion $U_d(U_p)$ for two holes on Cu(O)-sites, respectively, and a Coulomb repulsion $V = U_{pd}$ between nearest neighbor Cu-O pairs. This model, which is also known as Emery's model [11] , is able to describe a variety of situations, e.g. insulators with Mott-Hubbard and charge-transfer gaps.

$$H = \sum_{i,j,\sigma} \epsilon_{i,j} a^+_{i,\sigma} a_{j,\sigma} + \frac{1}{2} \sum_{i,j,\sigma,\sigma'} U_{i,j} n_{i,\sigma} n_{j,\sigma'}. \tag{3}$$

Throughout this work we use the hole picture, i.e. the $a^+_{i,\sigma}$ are creation operators for holes in copper $3d_{x^2-y^2}$ or oxygen $2p_x(2p_y)$ orbitals, respectively, and $n_{i,\sigma}$ are the

corresponding particle number operators. We use particle with the same meaning as holes. The vacuum state has no holes, and corresponds to $Cu^+$ and $O^{2-}$, i.e. all 3d and 2p states occupied. Besides the site diagonal terms $(\epsilon_{i,i}, U_{i,i})$, i.e. $(\epsilon_d, U_d)$ and $(\epsilon_p, U_p)$, we may also include the nearest neighbor repulsion $V = U_{pd}$ [21] . The hopping matrix element $\epsilon_{ij} = t_{pd} = 1$ is taken as unit of energy, and the appropriate phases are taken into account according to the symmetry of the wave functions. In certain cases also the hopping matrix element $t_{pp}$ between neighboring oxygen sites is taken into account.

## SINGLE-PARTICLE EXCITATIONS OF EXTENDED HUBBARD MODELS

There are a wide variety of experimental probes of condensed systems (XPS, UPS, BIS, EELS, etc.) [1] for which a theoretical description may be formulated simply in terms of a single-particle (-hole) propagator. In the particular case of transition metal oxides, these measured excitation spectra cannot be understood fully using conventionally calculated band structures. These discrepancies may however be understood to arise from correlation effects which are not properly treated in single particle band structure calculations. These features may most simply and successfully be handled within an impurity model [10] , where a single metal ion coordinated by the appropriate ligands models the crystal. This approach has the advantage of being simple enough to allow for a realistic treatment of many atomic orbitals with crystal-field effects etc. On the other hand, there are interesting questions concerning for example quasiparticle dispersion, i.e. width of bands, which cannot readily be considered within the impurity approach.

The model calculation presented here may be considered as a step from the impurity problem toward the crystal. Even with the restriction of the model to only a single orbital per site, the practical limit is at present reached with a cluster of only 4 $CuO_2$ units. This is a rather severe limitation because the discrete nature of the spectra of finite systems may cause difficulties in the interpretation of the calculated spectra. This problem is at least partially overcome through the use of modified periodic boundary conditions [22,23] . This consists of the inclusion of complex phase factors $\exp(i\phi)$ when a particle crosses the boundary of the cluster and enters again at the other side. Through this device it is possible by varying the angle $\phi$ to alter the set of allowed single particle momenta continuously. The accompanying energy shifts result in a filling in of the calculated spectra.

We begin with a qualitative discussion of the spectral function and of the main changes expected from correlation effects on the large energy scale. Figure 1(a) gives a sketch of the density of states for the 3-band model. For the undoped system the antibonding band is half-filled, that is the bandstructure is that of a metal. If we include the large Coulomb correlation on Cu this band is expected to split, forming a lower and upper Hubbard band (Fig. 1b). These 'bands' correspond to transitions $d^9 \rightarrow d^8$ and $d^9 \rightarrow d^{10}$, respectively.

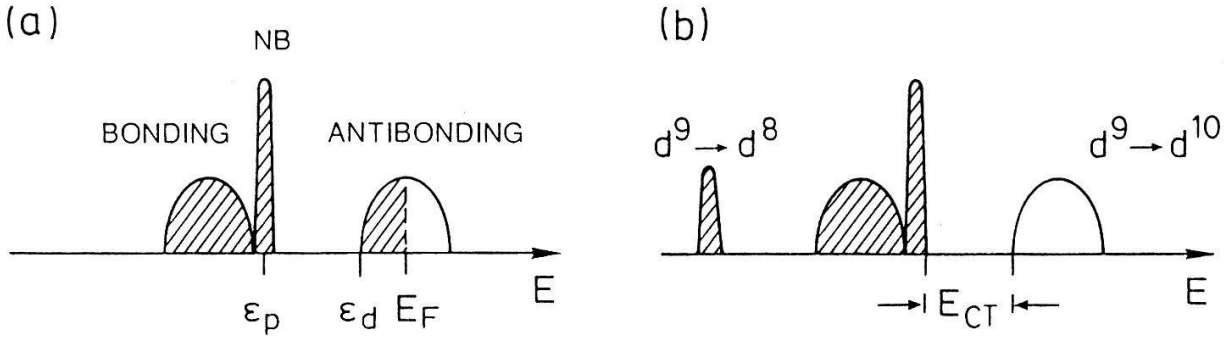


*Fig. 1:*
*(a) Sketch of density of states for the 3-band model. The antibonding band is half-filled in the undoped case ($d^9p^6$). The nonbonding band (NB) is dispersionless for $t_{pp} = 0$. (b) Sketch of Photoemission (shaded) and inverse PES in the presence of strong correlations on Cu (large $U_d$). The antibonding band is split into a lower and upper Hubbard band as a result of correlations. In the case $U_d \gg \epsilon$ shown here the lowest particle-hole excitations are across the charge transfer gap $E_{CT}$.*

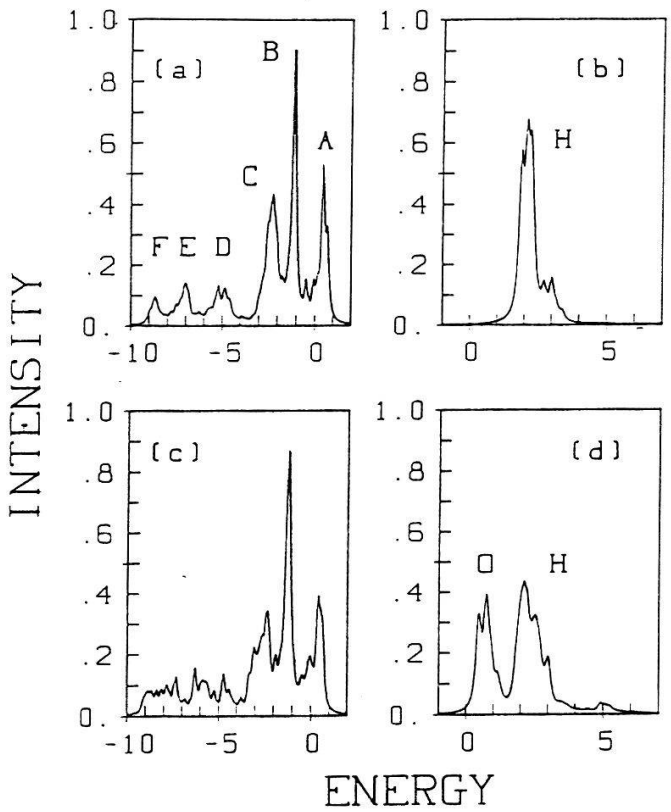


*Fig. 2:*
*Photoemission spectra for the parameters $\epsilon = 2.0$, $U_d = 6.0$, $U_p = 3.0$, $U_{pd} = 0.0$, with $t = 1.0$ taken as the unit of energy. Figures 2(a,b) show PES and inverse PES, respectively, for the undoped initial state. Figs. 2(c,d) represent a repetition of the same calculations starting from an initial state with one extra hole, which implies a doping concentration of 25%.*

The $d^8$ final state (2 holes on Cu) is shifted by an energy $\sim U_d$. Such a spectrum is characteristic for charge-transfer insulators [10,2] with a CT-gap $E_{CT}$.

Figure 2(a,b) shows typical photoemission and inverse photoemission spectra (PES) starting from the undoped ground state [18] . The parameters chosen are $\epsilon = 2.0$, $U_d = 6.0$, $U_p = 3.0$, $U_{pd} = 0.0$, with $t = 1.0$ taken as the unit of energy. All energy scales must be multiplied by $t_{pd} \sim 1.5eV$ to have energies in eV. This parameter set is representative for the values found in the constrained-density-functional approach [24] . The existence of a gap between the top of Fig. 2(a) and the bottom of Fig. 2(b) is consistent with an insulating ground state at half-filling, as expected. The structures B and C in PES (2a) derive from the nonbonding and bonding bands, respectively. A sharp and well separated $d^9 \rightarrow d^8$ satellite appears only for larger values for $U_d$ (see Fig. 3(b)). For the parameter set of Fig. 2 a more complicated structure D,E,F results due to a mixing with other final states, e.g. $d^{10}p^4$. This actually shows that the ground state fluctuates between $d^9p^6$ and $d^{10}p^5$ ($< n_d > \sim 0.7$ holes).

The most interesting feature, however, are the low-lying excitations A which have no correspondence in the bandstructure, and appear as result of correlations. This also implies an important modification of the picture as sketched in Fig. (1b). We will discuss these states below.

The most notable change in spectra (2c) and (2d) of the hole-doped system is the appearance of states in the inverse PES within the energy region corresponding to the gap at half-filling shown in Figs. 2(a) and (b). The emergence of these states upon doping is actually seen e.g. in XAS-experiments [2] . The existence of a pseudogap between these states and the upper Hubbard band H sets a lower limit for $\epsilon$.

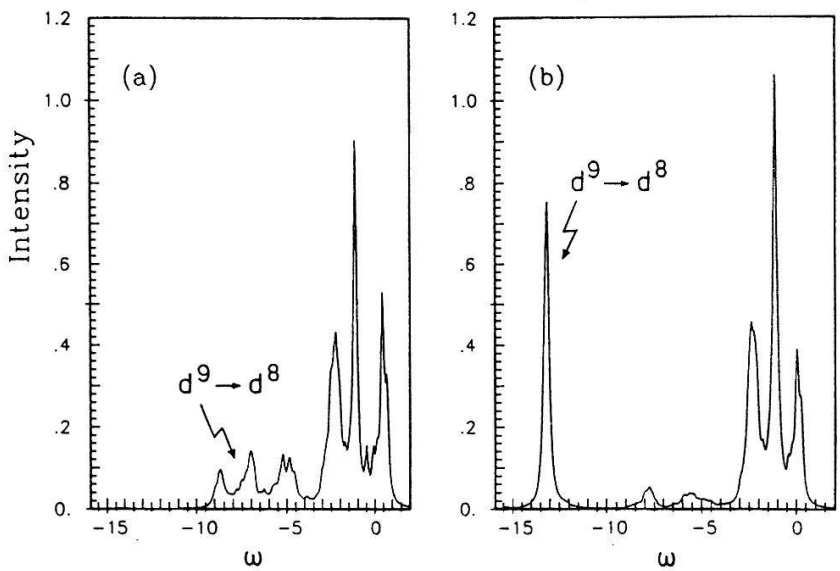


*Fig. 3:*
*(a) Photoemission spectrum as 2(a) in comparison to a PES (b) where $U_d$ was increased from 6 to 12. All other parameters as in Fig. 2.*

A further possibility for this type of calculation is illustrated in Fig. 4, where another example of an inverse photoemission spectrum for a hole-doped ground state is shown. In distinction to the previous case, electrons are now injected on Cu-sites or alternatively on oxygen-sites by an appropriate definition of the creation operator $a^+_{k\sigma}$ in the Greens function (2). The oxygen spectrum, Fig. 4, is related to an O1s absorption spectrum (XAS) [2,3]. It is evident that the upper Hubbard band has some oxygen character, because in the ground state $< n_d > \sim 0.7$. The 'oxygen related' gap states are strongly hybridized and have considerable Cu-character. Evidence for such a strong hybridization of the states close to the Fermi level has been found in recent photoemission experiments of the $Bi_2Sr_2CaCu_2O_8$ materials [25]. We also mention that the weights in a PES depend sensitively on what linear-combination e.g. of O-orbitals in a unit cell is chosen in the definition of $a^+_{\vec{k}}$.

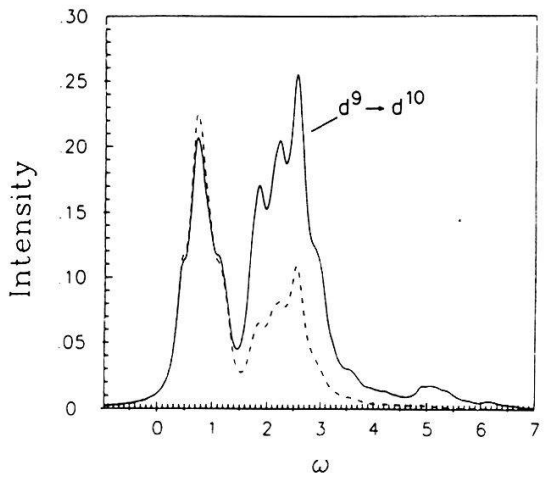


*Fig. 4:*
*Inverse photoemission for a hole-doped ground state. Electrons are injected on Cu-sites (solid line) or on O-sites (dashed curve). Same parameter set as for Fig. 2.*

## LOW-LYING SINGLE PARTICLE EXCITATIONS

A particularly interesting feature in Fig. 1 is as already emphasized the appearance of the low-lying excitations (A). They have no explanation in the bandstructure framework. In order to characterize these states we calculate the local singlet and triplet correlation functions

$$C_s = \sum_i < \psi^+_{si}\psi_{si} >, \tag{4}$$

$$C_t = \sum_i < \psi^+_{ti}\psi_{ti} >, \tag{5}$$

$$\psi_i = \frac{1}{\sqrt{2}}(d_{i\uparrow}P_{i\downarrow} \mp d_{i\downarrow}P_{i\uparrow}), \tag{6}$$

where the $-(+)$ sign refers to the local singlet (triplet). Here, the operator $P^+$ creates a hole in a symmetric linear combination of oxygen orbitals around a Cu site, i.e. the symmetric orbital has the same symmetry as $d_{x^2-y^2}$. For the lowest final state A (Fig.2) we find a large singlet correlation $C_s$ and almost vanishing triplet correlation function (Fig. 5), that is a strong antiferromagnetic correlation between an oxygen hole and its Cu-neighbors. Similar results for $C_s$ have been obtained by finite-temperature Monte-Carlo calculations [26] . These results support arguments given by Zhang and Rice [12] and also by Eskes and Sawatzky [27] . They argued that the singlet state

$$\psi_s^+|0>=\frac{1}{\sqrt{2}}(P_\downarrow^+ d_\uparrow^+ - P_\uparrow^+ d_\downarrow^+)|0> \tag{7}$$

formed by two holes in a $CuO_4$-cluster for $U_d \gg \epsilon \gg t$ and which is separated from the triplet and nonbonding states by

$$E_{st} = -8\,(\frac{t_{pd}^2}{U_d-\epsilon}+\frac{t_{pd}^2}{\epsilon}), \tag{8}$$

should also form the low-lying excitations of the $CuO_2$-planes. Equation (7) may also be seen as Heitler-London limit of a covalent bond

$$\psi_{cov}^+|0>=\left(a\, d_\uparrow^+ d_\downarrow^+ + \frac{b}{\sqrt{2}}(P_\downarrow^+ d_\uparrow^+ - P_\uparrow^+ d_\downarrow^+) + c\, P_\uparrow^+ P_\downarrow^+\right)|0> \tag{9}$$

formed out of the $d_{x^2-y^2}$ and the corresponding symmetric oxygen orbital.

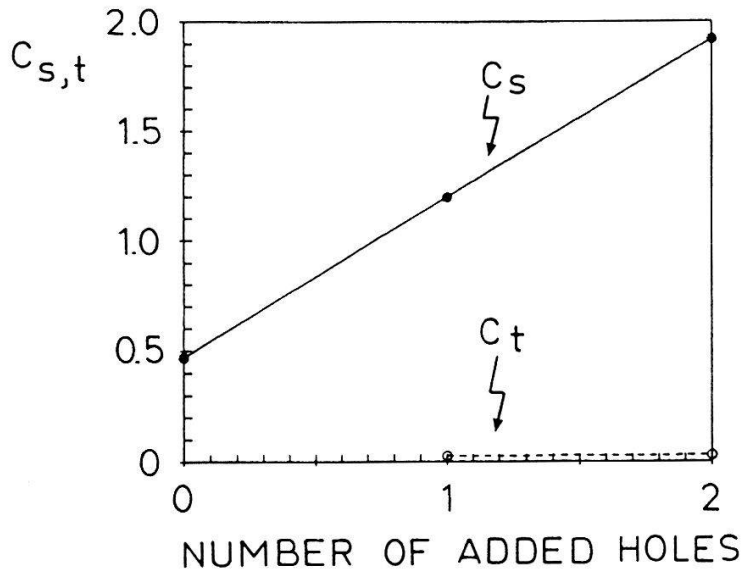


*Fig. 5:*
*Local singlet ($C_s$) and triplet ($C_t$) correlation functions in the ground state of the Emery model with 0,1, and 2 additional holes. Parameter set as for Fig. 2.*

Doping introduces holes into these low-lying states. This leads to a strong suppression of the antiferromagnetic order between Cu-sites,. which may be measured e.g. by the spin-spin correlation function between nearest neighbor Cu-sites

$$C_1 = \frac{1}{N} \sum_{i,\vec{\delta}} < S^z_{Cu}(\vec{r}_i + \vec{\delta}) S^z_{Cu}(\vec{r}_i) >, \tag{10}$$

$$C_2 = \frac{1}{N} \sum_{i,\vec{\delta}} < S^z_{Cu}(\vec{r}_i + \vec{\delta})\, n_O(\vec{r}_i + \vec{\delta}/2)\, S^z_{Cu}(\vec{r}_i) > . \tag{11}$$

Here $\vec{\delta}$ connects nearest neighbor Cu-sites. The second CF $C_2$ is particularly interesting because it measures the spin-correlation function between two Cu-neighbors only when an oxygen hole sits in between. With one additional hole, corresponding to a doping concentration of 25%, $C_1$ is strongly reduced, yet still antiferromagnetic. $C_2$ on the other hand is ferromagnetic [17] , that is the oxygen hole tends to align it's neighboring Cu-spins ferromagnetically when it moves through the crystal. Note that the correlation between Cu and the spin of the O-hole is antiferromagnetic, due to the singlet formation. This feature is similar to the frustration model of Aharony [28] , albeit the size of the local ferromagnetic correlation is much smaller than in their model [17] , which does not allow for hybridisation and the motion of the carriers.

## EFFECTIVE HAMILTONIAN FOR THE STRONG CORRELATION LIMIT: t-J MODEL

It was emphasized by Anderson that the low-energy physics of the $CuO_2$-planes in high-$T_c$-superconductors is contained in the single-band Hubbard model:

$$H = -t \sum_{\langle i,j \rangle} \left( c^+_{i,\sigma} c_{j,\sigma} + c^+_{j,\sigma} c_{i,\sigma} \right) + U \sum_i n_{i,\uparrow} n_{i,\downarrow}. \tag{12}$$

The t-J-model is derived from the Hubbard Hamiltonian in the limit $t/U \ll 1$. By canonical transformation doubly occupied configurations are eliminated [29,30,31] leading to the following Hamiltonian up to order $t^2/U$

$$\begin{aligned} H_{tJ^*} = -t \sum_{i,j,\sigma} c^+_{i,\sigma} c_{j,\sigma} + \frac{t^2}{U} \sum_j \sum_{\delta,\delta'} (& c^+_{j+\delta\uparrow} c^+_{j\downarrow} c_{j\downarrow} c_{j+\delta'\uparrow} + c^+_{j\uparrow} c^+_{j+\delta\downarrow} c_{j+\delta'\downarrow} c_{j\uparrow} \\ & + c^+_{j+\delta\uparrow} c^+_{j\downarrow} c_{j+\delta'\downarrow} c_{j\uparrow} + c^+_{j\uparrow} c^+_{j+\delta\downarrow} c_{j\downarrow} c_{j+\delta'\uparrow}), \end{aligned} \tag{13}$$

where $j+\delta$ and $j+\delta'$ are nearest neighbors of $j$, respectively. It is understood here that creation and annihilation operators are restricted to the space without double occupancy. The $t^2/U$-terms describe a hop from $j+\delta$ to $j+\delta'$ via a virtual intermediate state with a double occupancy at $j$. The t-J-Hamiltonian with $J = 4t^2/U$ follows from the 2-site contributions ($\delta = \delta'$) after rewriting in terms of spin and number operators.

$$H_{tJ} = -t \sum_{i,j} c^+_{i,\sigma} c_{j,\sigma} + J \sum_{\langle i,j \rangle} \left( \vec{S}_i \cdot \vec{S}_j - \frac{n_i n_j}{4} \right). \tag{14}$$

The 3-site terms ($\delta \neq \delta'$) only contribute in the presence of a hole. These terms are frequently neglected, which is a valid approximation close to half-filling when one is interested in e.g. the ground state energy, where the corrections are of the order $\delta_h J$ with $\delta_h$ being the concentration of holes. Yet for our problem, i.e. the propagation of a hole, it is not at all obvious that they can be neglected. This is easily seen when acting with the 3-site terms of Eq.(3)

$$H_J^{(3)} = -\frac{t^2}{U} \sum_{j,\sigma} \sum_{\delta \neq \delta'} \left( c^+_{j+\delta,\sigma} n_{j,\bar{\sigma}} c_{j+\delta',\sigma} - c^+_{j+\delta,\sigma} c^+_{j,\bar{\sigma}} c_{j,\sigma} c_{j+\delta',\bar{\sigma}} \right) \tag{15}$$

onto the Néel-state with a single hole. The effect of the first term of $H_J^{(3)}$ is to propagate the hole on it's sublattice and thereby leaving the Néel order unchanged! The second term describes also a next-nearest neighbor hop but with an associated spin flip.

Zhang and Rice [12] argued that the low lying excitation spectrum of the Emery model [11], which gives a more realistic description for the electronic structure of the $CuO_2$-planes in HTSC's, can be mapped on the t-J-model. This correspondence is considered valid in the limit that $U_{Cu}$ and the level spacing $\epsilon = \epsilon_p - \epsilon_d$ between Cu($d_{x^2-y^2}$) and O($p_\sigma$) orbitals is large compared to the hybridisation $t_{pd}$. In this limit the superexchange is given by

$$J = \frac{4t_{pd}^4}{\epsilon^2} \left( \frac{1}{U_d} + \frac{1}{\epsilon} \right), \tag{16}$$

while the hopping matrixelement describing the motion of a singlet is of the order [12]

$$t \sim \frac{t_{pd}^2}{\epsilon}. \tag{17}$$

An alternative derivation of a generalized t-J model has been proposed recently by Ramsak and Prelovsek [32].

We note that the upper and lower Hubbard band of the effective single-band Hubbard model corresponds to structures (A) and (H) in the spectra of the Emery model. The effective U being of the order of the charge- transfer gap. We will return below to the question of the equivalence of the low-lying excitations of the Emery model and those of the t-J model.

## SPECTRAL FUNCTION IN ONE DIMENSION

The spectral function for a hole moving in a classical Neel-state (J=0), that is moving via the restricted hopping only, has been worked out by Brinkman and Rice [33]. The single particle Greens function for this case

$$G(\omega) = \frac{1/\omega}{1 - \frac{z}{z-1}[\frac{1}{2} - \sqrt{\frac{1}{4} - (z-1)\frac{t^2}{\omega^2}}]} \tag{18}$$

describes a k-independent continuum, i.e. the Greens function in real space is given by $G_{ij}(\omega) = \delta_{ij}G(\omega)$. In 1D, i.e. the number of nearest neighbors is z=2, their retraceable path approximation gives a rigorous result for a hole moving in a classical Neel-state.

The inclusion of J within the same framework [34] yields in 1D a k-dependent deformation of this continuum

$$G(k,\omega) = \frac{1}{J\cos 2k + \sqrt{(\omega - J\cos 2k)^2 - 4t^2}}, \tag{19}$$

which results from the spin-flip terms in the Hamiltonian (15). The edge of the continuum is at $\omega_0^{\pm} = \pm 2t + J\cos 2k$ neglecting the Ising part of $H_J$ which leads merely to a shift of the edge in one dimension. We note that in this approximation the width of the dispersion is overestimated by a factor 2 as compared to the numerical result in the complete Hilbert space [35] .

To illustrate the importance of the 3-site terms (14) we compare in Fig. 6 the results for the lower edge of the continuum for 3 cases: the 1-band Hubbard model, the t-J and the $t - J^*$-model. The latter model includes the 3-site terms. The inclusion of these terms improves the quantitative agreement with the Hubbard model significantly. Yet as the dispersion is not significantly changed by including these terms, they seem not to be particularly relevant for the propagation of carriers.

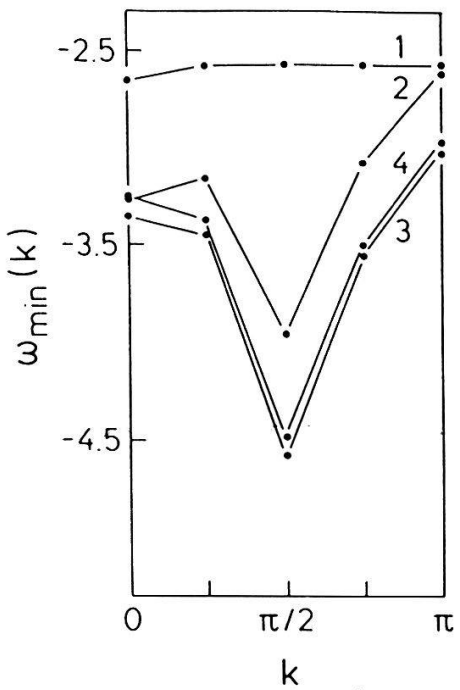


*Fig. 6:*
*k-dependence of the state with lowest energy in one dimension (N=8) for various models: (1) Ising ,(2) $t - J$, (3) $t - J^*$, and (4) the single-band Hubbard model. The energy for J=0 was subtracted for each k-value to account for finite size effects. The difference is given in units of J, which was 0.2 in these calculations.*

We will not describe here the interesting changes of these continuous spectra when one starts from the exact singlet ground state as initial state in (2) instead. Numerical results for the k-dependence of these spectra are given by Szczepanski et al [35] . Analytical studies on the role of zero point motion in the ground state have been performed by Brenig and Becker [36] and by Ziegler and Horsch [34] .

## SPECTRAL FUNCTION IN TWO DIMENSIONS

The density of states $A(\omega)$ of a single hole in the t-J model for $J = 0$ is shown in Fig. 7 . The Néel state has been taken as initial state. Brinkman and Rice predicted a narrowing of the band for this case, as compared to e.g. the motion of a hole in a ferromagnetic background. The lowest spin-1/2 states lie at $\omega_0 \approx -3.45\,t$ for N=16, which is very close to the band edge $\omega_0 = -2\sqrt{3}\,t$ in the retraceable path approximation Eq.(18). The band tail extending to $-4t$ is formed by high spin states, which have small spectral weight.

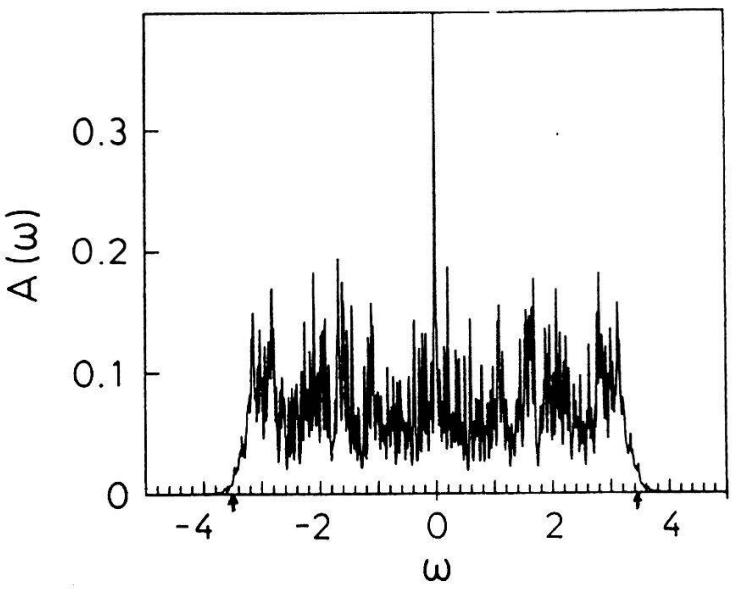


*Fig. 7*
*Density of states of single hole in a classical Neel-state in 2D. $A(\omega)$ was calculated in the t-J model for J=0 numerically for a $4 \times 4$ unit cell. The arrows indicate the edges of the Brinkman-Rice continuum at $\omega = \pm 2\sqrt{3}t$.*

The $S = 1/2$-states become lowest when the antiferromagnetic coupling between the spins exceeds a critical value. Exact diagonalization studies showed the existence of a critical value of $J_c$ for finite systems [37,38] above which the fully spin-polarized state, which is stable according to Nagaoka's theorem [39] in the limit $J = 0$, becomes unstable. For 16 sites the ferromagnetic state becomes unstable for $J_c^{min} \approx 0.06$, while above $J_c^{max} \approx 0.075$, the ground state already has spin $S = 1/2$. As an estimate for the thermodynamic limit one finds $J_c \approx 0.005$ when neglecting $H_J^{\perp}$. [40] That is, in the physically interesting regime the low-energy states have low spin (S=1/2).

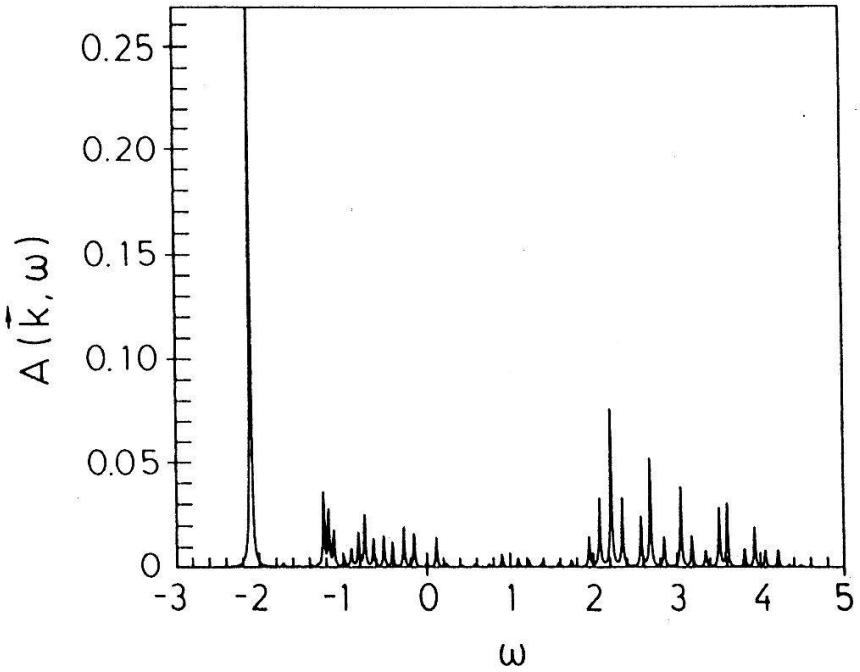


*Fig. 8*
*Spectral function $A(\vec{k},\omega)$ at $\vec{k} = (\frac{\pi}{2}, \frac{\pi}{2})$ for a single hole inserted into the exact singlet ground state of the Heisenberg antiferromagnet in 2D ($N = 4 \times 4$ and $J/t$=0.2).*

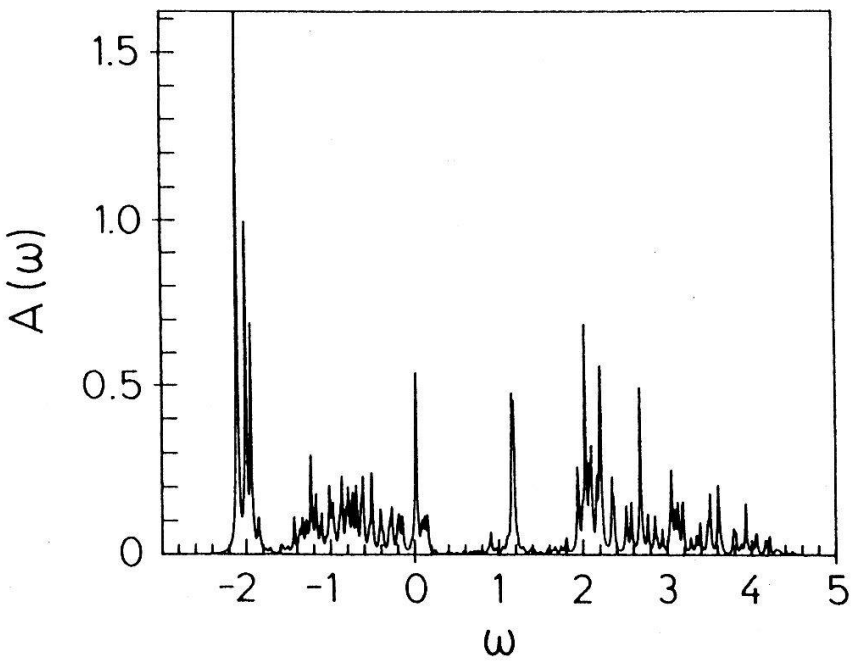


*Fig. 9:*
*Momentum integrated spectral function (density of states). Same parameters as Figure 8.*

A different picture emerges if one considers the spectral function of a hole moving in a spin fluctuating background $\psi_0$ for finite J [18,35]. A typical spectrum for $A(\vec{k},\omega)$ at $\vec{k} = \left(\frac{\pi}{2}, \frac{\pi}{2}\right)$ is shown in Fig. 8 for $N = 16$. The form of this spectrum with a peak at the low-energy side of a continuum of width 7t is similar to spectra at other $\vec{k}$-values for $N = 16$ and $N = 18$, except for those at the special points $\vec{k} = (0,0)$ and $(\pi,\pi)$.

The momentum integrated spectral function starting from the singlet ground state of the Heisenberg model is shown in Fig. 9. The set of peaks, which arise from different $\vec{k}$-values at the bottom of the continuum, appear well separated from the incoherent part of the spectrum. The separation is of the order of 2J and might be related to a density of states effect of the spin excitations as suggested by Kane et al. [41] The depletion of $A(\omega)$ in the interval $0 \leq \omega \leq 2t$ is already present for $J \to 0$ and is a signature of the singlet ground state. It is not seen in calculations starting from the classical Neel-state. The peak at $\omega \approx 1$ stems from the spectrum at $\vec{k} = (\pi,\pi)$. The dispersion of this quasiparticle (QP) band is drawn in Fig. 10 for systems with $N = 16$ and 18 sites and different values of $J$, after subtracting a momentum independent, but $J$-dependent constant $E_M$. The lowest energies are found close to the Fermi surface of the noninteracting case, i.e., $\vec{k} = \left(\frac{\pi}{2}, \frac{\pi}{2}\right)$ and $(\pi, 0)$. The center of the QP band, i.e., the mean of the QP energies at $\vec{k} = (\pi,\pi)$ and $\left(\frac{\pi}{2}, \frac{\pi}{2}\right)$ for 16 sites, is given by $E_M(J) = -3.28 + 5.09\, J^{0.81}$ for $J$ between 0.04 and 0.5. A very similar dependence is found for the 18 site system. The solid line in Fig. 10 shows the function

$$E_{\vec{k}} = J\left[\frac{1}{2}\left(\cos k_x + \cos k_y\right)^2 - 1\right]. \tag{20}$$

The form of this dispersion $\omega_{\vec{k}}$ is related to an effective next-nearest neighbor hopping. The dependence of the QP bandwidth $W$ on $J$ is more accurately described by $W(J) = -0.23 + 2.66\, J^{0.91}$ for 16 sites and $J$ between 0.04 and 0.5. The negative intercept indicates two conflicting mechanisms: (a) the coherent motion via spin-flip and (b) higher order processes in the hopping [42]. For larger values for J the spin-flip process is dominant. The "reversed" dispersion is actually observed for $J \leq 0.06$, as well as in the pure Ising case. We note that the uncertainty in both the choice of the upper limit of the QP dispersion and the $J$-dependence of the QP bandwidth made a reliable establishment of the behaviour in the thermodynamic limit impossible. On the basis of our data we therefore cannot decide, whether the bandwidth is linear in $J$ or obeys a sub-linear form as proposed by Gros and Johnson. [43]

Our finding of a well defined peak at the bottom of the continuum confirms the dominant pole approximation in the work of Kane, Lee and Read [41] in their extension of the approach of Schmitt-Rink et al [44]. The emergence of undamped low-energy excitations may be understood as consequence of the string energy associated with the motion of a hole in 2D, which survive when spin-wave excitations are included. Surprisingly their perturbative treatment about the Ising limit, i.e., considering the anisotropy $\alpha = J^{\perp}/J^{z}$ as small parameter, gives the proper width for the quasiparticle band at the isotropy point ($\alpha = 1$). In the retraceable path approximation one obtains

the same dispersion relation, yet the width is overestimated by a factor of 2, as in 1D. We emphasize that the spectral weight of the quasiparticle peak is large over the whole Brillouin zone except at the special points $\vec{k} = (0,0)$ and $(\pi,\pi)$ where the weight is rather small and other states dominate the spectrum.

We finally mention that the features of Fig. 8 in particular the well separated quasiparticle peak, are hardly changed if we perform the same calculations for the XY-Hamiltonian.

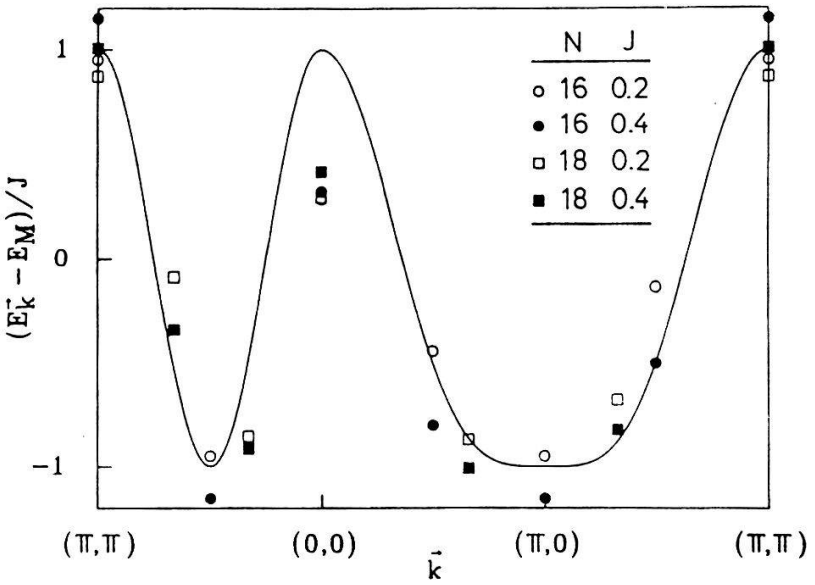


*Fig. 10:*
*The dispersion of the quasiparticle peak in the spectral function (2D) is plotted along the principle axis of the Brillouin zone, after subtracting a momentum independent constant $E_M$ and normalization by J. The numerical results for N=16 and 18 sites are included for two different values for of the interaction strength J/t=0.2 (0.4). The dispersion $E_{\vec{k}}$ , Eq. (20), is drawn as solid line.*

## EQUIVALENCE OF LOW-LYING EXCITATIONS OF THE EMERY MODEL AND THE t-J MODEL.

According to Zhang and Rice the separation between singlet and triplet excitations should persist in the $CuO_4$-lattice. Recently Prelovsek and coworkers [32] have supported this point of view by studying small clusters. If we assume this to be the case, then we expect that the singlet states will form a incoherent band of width 7t and a quasiparticle peak at the low-energy side of this continuum as in the t-J model. This structure should be still separated from the triplet excitations.

Numerical studies are still limited to supercells with $4CuO_2$-units which corresponds to a 4-site t-J model. The low-lying excitations in the Emery model have been identified according to their singlet and triplet character. We find that the singlet structures are below the triplet excitations and there exists a one-to-one cor-

respondence to the spectra of the t-J model for the different $\vec{k}$-values. To be more specific, for e.g. $\vec{k} = (\pi, 0)$ there are only two peaks in the t-J model for $N = 2 \times 2$. These peaks are separated by an energy of 7t, this is by coincidence precisely the width of the continuum for the larger system ($N = 4 \times 4$) in the t-J model. The corresponding low-energy structures in the Emery model have singlet character and are below the triplet states.

The correspondence is clear for large values for $U_d$ and $\epsilon$ but seems to persist into the realistic parameter regime. We finally mention that finite $t_{pp}$ does not destroy this result. Actually the singlet is further stabilized, which has also been reported by others [45] .

## SUMMARY

The most notable structures in the photoemission spectra of the Emery model are besides the satellites at high energy the appearance of low-energy states below the band-like states (Zhang-Rice singlet). Occupation of these states leads to the frustration of antiferromagnetic order between Cu-sites. In the hole-doped systems these states appear in the charge-transfer gap and are seen in inverse PES. Remnants of the charge-transfer gap are expected to remain as pseudo-gap for sufficiently large p-d level separation. The spectra calculated for realistic parameters also show that the states in the CT-gap are strongly hybridized, i.e., additional holes do not exclusively reside on oxygen. We finally mention that the energetic position of the satellites calculated for parameters taken from the constrained-density-functional approach are in good agreement with experiment.

New puzzles are posed, however, by the recently found electron doped superconductors with $CuO_2$-planes [46] , e.g.$Nd_{2-x}Ce_xCuO_4$. In the framework of the Emery model these electrons would go into the upper Hubbard band (H in Fig.2) corresponding to the formation of $Cu^+$. The edge of the Hubbard band would be pinned to the Fermi level. The low-energy states found in inverse photoemission (XAS) in these compounds [2] could be taken as confirmation of this picture. Yet these states have also been interpreted differently [2] , and furthermore there is still no clear experimental evidence for the substantial increase of $Cu^+$. This might indicate the necessity to extend the model.

The motion of a carrier (hole) strongly interacting with the spins of a Heisenberg antiferromagnet was studied in detail in the case of the t-J model. Our central finding is a coherent quasiparticle band with dispersion $E_{\vec{k}} \sim \frac{J}{2}(\cos k_x + cos k_y)^2$ and $S = 1/2$, which emerges at the low-energy side of a broad incoherent spectrum of width 7t.

## ACKNOWLEDGEMENTS

I am particularly grateful to W. Stephan, M. Ziegler, K.v.Szczepanski, W. von der Linden who have contributed to this work, and to P. Fulde, J. Fink, A. Muramatsu, P. Prelovsek, and J. Zaanen for many stimulating discussions.

REFERENCES


1. J. C. Fuggle, J. Fink, and N. Nücker, Int. J. Mod. Phys. B1,1185 (1988) and references therein.
2. J. Fink et al. in 'Earlier and recent aspects of Superconductivity', ed. K.A. Müller and G. Bednorz; Springer Series of Solid-State Sciences.
3. F. J. Himpsel et al., Phys. Rev. B38,11946 (1988).
4. T. Takahashi et al., Nature 334,691 (1988).
5. R. Manzke, T. Buslaps, R. Claessen, and J. Fink, Europhys. Lett. 9, 477 (1989).
6. J. M. Imer et al., Phys. Rev. Lett. 62,336 (1989).
7. P. W. Anderson, Science 235,1196 (1987), Proceedings of the International School of Physics 'Enrico Fermi', July 1987, (North Holland, Amsterdam,1989), and Physics Reports 184, 195 (1989).
8. P. Fulde, Physica C153-155,1769 (1988).
9. J. Zaanen, O. Jepsen, O. Gunnarsson, A.T. Paxton, and O. K. Andersen, Physica C153-155,1636 (1988).
10. J. Zaanen, G.A. Sawatzky, and J.W. Allen, Phys.Rev.Lett. 55,418 (1985), J. Zaanen, C. Westra, and G. A. Sawatzky, Phys.Rev. B33,8060 (1986).
11. V. J. Emery, Phys. Rev. Lett. 58,2794 (1987).
12. F. C. Zhang and T. M. Rice, Phys.Rev. B37,3759 (1988).
13. See e.g. 'Dynamics of Magnetic Fluctuations in High- Temperature Superconductors', ed. G. Reiter, P. Horsch, and G. Psaltakis, (Plenum, New York, 1990).
14. R. Haydock, V. Heine, and M. J. Kelly in Solid State Physics, Vol.35, edited by H. Ehrenreich, F. Seitz, and D. Turnbull (Academic, New York, 1980).
15. O. Gunnarsson and K. Schönhammer, Phys. Rev. B31, 4815 (1985).
16. C.A. Balseiro, A.G. Rojo, E.R. Gagliano, and B. Alascio, Phys. Rev. B38, 9315 (1988).
17. P. Horsch and W.H. Stephan, in 'Interacting Electrons in Reduced Dimensions', ed. by D. Baeriswyl and D. Campbell (Plenum,New York,1989).
18. P. Horsch, W.H. Stephan, K. v. Szczepanski, M. Ziegler, and W.v.d. Linden, Physica C 162-164, 783 (1989).
19. W.E. Pickett, Rev. Mod. Phys. 61, 433 (1989).
20. M. S. Hybertsen and L. F. Mattheiss, Phys. Rev. Lett. 60,1661 (1988).
21. W.H. Stephan, W. von der Linden, and P. Horsch, Phys. Rev. B39, 2924 (1989) and Int. J. Mod. Phys. B1, 1005 (1988).
22. R. Jullien and R. M. Martin, Phys. Rev. B26,6173 (1982).

23. A. M. Oles, G. Treglia, D. Spanjard, and R. Jullien, Phys. Rev. B32,2167 (1985).

24. M. S. Hybertsen, M. Schlüter and N. E. Christensen, Phys. Rev. B 39, 9028 (1989); A.K. McMahan, R.M. Martin, and S. Satpathy, Phys. Rev. B38, 6650 (1988); E.B. Stechel and D.R. Jennison, Phys. Rev. B40, 6919 (1989).

25. R.S. List et al., Physica C 159, 439 (1989).

26. G. Dopf, A. Muramatsu, and W. Hanke, to be published.

27. H. Eskes and G.A. Sawatzky, Phys. Rev. Lett. 61, 1415 (1988).

28. A. Aharony, R. J. Birgeneau, and M. A. Kastner, Int.J.Mod.Phys. B1,649 (1988).

29. L.N. Bulaevskii, E.L. Nagaev, and D.L. Khomskii, Sov. Phys. JETP 27, 836 (1968).

30. J.E. Hirsch, Phys. Rev. Lett. 54, 1317 (1985).

31. J. Zaanen and A.M. Oles, Phys. Rev. B37, 9423 (1988).

32. A. Ramsak and P. Prelovsek, Phys. Rev. B40, 2239 (1989).

33. W.F. Brinkman and T.M. Rice, Phys. Rev. B2, 796 (1970).

34. M. Ziegler and P. Horsch, unpublished.

35. K.J. von Szczepanski, P. Horsch, W. Stephan, and M. Ziegler, Phys. Rev. B41, February (1990).

36. W. Brenig and K.W. Becker, preprint 1989.

37. J. Bonca, P. Prelovsek, and I. Sega, Phys. Rev. B 39, 7074 (1989).

38. D. Poilblanc, Phys. Rev. B 39, 140 (1989) and W. von der Linden, private communication.

39. Y. Nagaoka, Phys. Rev. 147, 392 (1966).

40. B.I. Shraiman and E.D. Siggia, Phys. Rev. Lett. 60, 740 (1988).

41. C.L. Kane, P.A. Lee, and N. Read, Phys. Rev. B 39, 6880 (1989).

42. S.A. Trugman, Phys. Rev. B 37, 1597 (1988).

43. C. Gros and M.D. Johnson, Phys. Rev. B40, 9423 (1989).

44. S. Schmitt-Rink, C.M. Varma, and A.E. Ruckenstein, Phys. Rev. Lett. 60, 2793 (1988).

45. H. Eskes, G.A. Sawatzky, and L.F. Feiner, Physica C160, 424 (1989).

46. Y. Tokura, H. Takagi, and S. Uchida, Nature 337, 345 (1989).